Examination of thermalization of quarkonia at energies available at the CERN Large Hadron Collider

Deekshit Kumar,[1,*] Nachiketa Sarkar,[2,†] Partha Pratim Bhaduri,[1,3,‡] and Amaresh Jaiswal[2,§]

[1]*Homi Bhabha National Institute, Anushakti Nagar, Mumbai 400094, India*
[2]*School of Physical Sciences, National Institute of Science Education and Research,*
An OCC of Homi Bhabha National Institute, Jatni 752050, India
[3]*Variable Energy Cyclotron Centre, 1/AF Bidhan Nagar, Kolkata 700064, India*

We analyze the relative yields of different bottomonia and charmonia states produced in Pb-Pb, *p*-Pb, and high multiplicity *p*-*p* collisions at the CERN Large Hadron Collider, within a semiclassical grand canonical ensemble approach. The underlying assumption is the early thermalization and subsequent freeze-out of these heavy hadrons resulting in their chemical freeze-out at a temperature of approximately 230 MeV, significantly higher than that of light and strange hadrons. The systematic dependence of the freeze-out temperature on the collision centrality is also investigated in detail.

I. INTRODUCTION

Quarkonia are the bound states of a heavy quark (Q) and its antiquark ($\bar{Q}$). The bound state of a charm (bottom) quark and its antiquark is called charmonium (bottomonium). The binding is believed to be hindered in the presence of a thermally deconfined medium, in a process analogous to the Debye screening in an electromagnetic plasma [1]. Since a thermalized partonic medium is likely to be formed in relativistic heavy-ion collisions, but is not concretely established in proton-proton (*p*-*p*) and proton-nucleus (*p*-*A*) collisions, the production yield of the quarkonium states is expected to be systematically different in the two cases. Suppression of heavy quarkonium states is believed to be a promising diagnostic probe of the properties of the hot and dense medium created in high-energy heavy-ion collisions [2–6].

If quark-gluon plasma (QGP) is formed in the collision zone, the confining potential of heavy quark-antiquark pairs is expected to be screened by the color charges leading to the in-medium modification of the quarkonium spectral functions. In addition, the medium-induced imaginary potential of the quarkonium system, modeled via the inelastic scattering with hard partons, leads to the thermal broadening of their in-medium width, at any finite temperature. These in-medium effects have been intensely studied based on lattice quantum chromodynamics (QCD) and effective field theories of QCD [7,8]. The resulting dissociation (or melting) of the quarkonium states in a hot plasma depends on the temperature, with loosely bound states melting earlier than the strongly bound ones. Quarkonium dissociation is thus expected to occur sequentially, reflecting the increasing values of their binding energies [9,10]. This leads to the characteristic sequential suppression pattern of different quarkonium states in heavy ion collisions, compared to their production in *p*-*p* collisions.

Experimentally charmonium production in heavy-ion collisions was measured at the CERN Super Proton Synchrotron (SPS) [11,12], the BNL Relativistic Heavy Ion Collider (RHIC) [13–15], and the CERN Large Hadron Collider (LHC) [16–24]. The systematic difference in the production pattern between nucleus-nucleus (*A*-*A*) collisions and *p*-*p* collisions is quantified by the nuclear modification factor (R_{AA}), defined as the ratio between the quarkonium yield in nuclear collisions and the yield in *p*-*p* collisions scaled by the number of binary nucleon-nucleon collisions. At the LHC, suppression of J/ψ production in nuclear collisions is weaker than the measurements at lower energies. In central collisions at LHC, the R_{AA} is much larger than at RHIC energy for low-p_T J/ψ. The p_T dependence of R_{AA} is also significantly different at RHIC and LHC. At RHIC, the p_T dependence is rather flat, but a clear decreasing trend with increasing p_T is observed at LHC. Comparison of the p_T dependence of the inclusive J/ψ R_{AA} in various rapidity windows also exhibits the decreasing trend with more suppression at higher rapidities. These observations are commonly attributed to the significant regeneration of the charmonium states at low p_T, from the initially deconfined and uncorrelated $c, \bar{c}$ pairs. Regeneration is more important at higher energies due to the larger amount of $c\bar{c}$ pairs present in the medium.

---

*deekshitkumarvecc@gmail.com
†nachiketa@niser.ac.in
‡Corresponding author: partha.bhaduri@vecc.gov.in
§a.jaiswal@niser.ac.in

In the bottomonium sector, measurements at the LHC are pioneered by the CMS Collaboration, with the observation of strong suppression of the $\Upsilon(1S)$ state in Pb-Pb collisions [25]. The production of the excited $\Upsilon(2S)$ state suffered a much stronger suppression. The $b\bar{b}$ production cross section is much lower than that of $c\bar{c}$, owing to their large mass. Bottomonium states are thus expected to be much less affected by the regeneration effect [26]. Attempts were also made to measure the nuclear modification factors in proton-nucleus (*p-A*) collisions at LHC, where formation of a deconfined plasma phase was not expected prior to the LHC measurements. Data indicate a significant modification of the $\Upsilon(1S)$ production at midrapidity and forward rapidity, in accordance with the expectations from the initial state effects. However, a stronger suppression is observed at backward rapidity, unaccountable by the known initial state effects. Additionally, excited states were seen to undergo stronger suppression, analogous to the pattern observed in *A-A* collisions. While R_{AA} is an useful observable to look for signals of medium formation in nuclear collisions, it is not the most appropriate quantity to study thermal physics. In the literature, more popular choices to address the issue of thermalization include the measurement transverse momentum (p_T) spectra and the elliptic flow (v_2), the second Fourier coefficient of the azimuthal anisotropy. In literature, the measured p_T spectra are analyzed within hydrodynamics inspired blast wave model to address the issue of the degree to which heavy quarks thermalize in the fireball and inherit the collective expansion of the medium. In Ref. [27], the possible thermal features of charmonium production were first pointed out by analyzing the p_T spectra of J/ψ (and ψ') mesons in $\sqrt{s_{NN}} = 17.3$ GeV Pb-Pb collisions at SPS. Subsequently the p_T distribution of J/ψ mesons measured at RHIC [28] and LHC [29] have also been analyzed within such a boosted thermal model framework. The underlying assumption in such analyses is the coincidence of the kinetic freeze-out temperature with that of chemical freeze-out due to negligible rescattering cross sections of charmonia in the hadronic phase. For bottomonia, Υ p_T spectra are currently available from the CMS Collaboration in $\sqrt{s_{NN}} = 2.76$ TeV Pb-Pb collisions, for 0–100% centrality [30]. Whether these spectra are in agreement with a blast wave model description is difficult to judge [31]. Recent measurements by both CMS and ALICE Collaborations in $\sqrt{s_{NN}} = 5.02$ TeV Pb-Pb collisions at LHC indicate a smaller v_2 of $\Upsilon(1S)$ states [32,33] than the one measured for inclusive J/ψ [34–36] mesons by the ALICE Collaboration. The measured $v_2(p_T)$ of the inclusive J/ψ mesons can be explained up to large p_T, using a transport model incorporating the state-of-the-art *c*-quark phase space distributions [37] into the regeneration process of charmonia. On the other hand, the v_2 of the Υ mesons was found to be consistent with zero over the measured p_T range. Within the associated uncertainty, the data can be explained both within models [26,38,39] which do not consider the *b* quark thermalization (and hence negligible regeneration) in the fireball or within the blast wave model framework [31] that assumes a scenario in which *b* quarks thermalize and the Υ mesons inherit the collective expansion of the medium. Hence neither of the possibilities can be ruled out.

In Ref. [40] the authors addressed the issue of quarkonium thermalization at LHC by analyzing the relative yields of different bottomonium states in $\sqrt{s_{NN}} = 2.76$ TeV Pb-Pb collisions, using then available data. The observed sequential suppression of the Υ family of mesons, as measured by the CMS Collaboration, was interpreted as the system being in thermal equilibrium in the fireball before freezing out. All the $Q\bar{Q}$ pairs present in the fireball are assumed to be produced in the initial hard scattering and eventually thermalize with the medium due to interaction. The production of heavy quark pairs is negligible at any conceivable plasma temperature. A simple dimensional analysis involving multiple scales including heavy quark mass M_Q and temperature T indicates that the net production rate of quarkonia at thermal equilibrium may be obtained by studying the spectral density of quarkonium states in thermal equilibrium. Lattice QCD simulations indicate increase in the decay width of the quarkonium states, Γ, at any finite T. The width is interpreted as the inclusive rate of all unbinding reactions in which a quarkonium state disintegrates into unbound $Q\bar{Q}$ pairs. Moreover, at LHC energies, one also needs to account for the reverse recombination rate that can be estimated from the dissociation process via the principle of detailed balance.

Note that large values of $\Gamma(T)$ would imply different bound and unbound $Q\bar{Q}$ states reaching thermal equilibrium with each other over a very short time. Production dynamics of the quarkonium states in nuclear collisions, where a thermalized partonic medium is anticipated, is thus entirely different than that in elementary *p-p* collisions. Different quarkonium states would continue to be in thermal equilibrium, until Γ falls below the expansion rate of the fireball and these heavy mesonic systems freeze out. This adopted picture of quarkonia production and evolution is similar in spirit with the statistical hadronization model (SHM) of quarkonia production. In this picture all the $Q\bar{Q}$ pairs are assumed to be produced in primary hard collisions and their total number remains conserved until hadronization. The number of $Q\bar{Q}$ pairs is thus effectively decoupled from the thermal description of the heavy quark hadronization at the QCD phase boundary, where charmonia (bottomonia) are formed from charm (bottom) quarks according to statistical weights evaluated at the chemical freeze-out. Apart from this nonthermal scale of the total number of charm quarks, the other parameters of the statistical hadronization scheme are the thermal parameters in a grand canonical description of the fireball. They are well constrained by the chemical freeze-out analysis of the light hadrons. Thus in SHM the quarkonia are believed to have a chemical freeze-out temperature of $T_f \simeq 156$ MeV, the same as all other hadrons. The so-called SHM for charmed hadrons (SHMC) provides a reasonable description of charmonium production [41–43] in nuclear collisions. The same model can also describe the relative production of $\Upsilon(1S)$ and $\Upsilon(2S)$ mesons in $\sqrt{s_{NN}} = 2.76$ TeV Pb-Pb collisions [44]. However, in contrast to SHM, in the present model the heavy quarkonia states are not made to undergo chemical freeze-out at same temperature as for light hadrons. Instead the chemical freeze-out of these heavy mesons is fixed by the available data, from the relative yield of different quarkonium states in Pb-Pb collisions.

Assuming all the quarkonium states to be in complete equilibrium with the fireball, their equilibrium densities are obtained in terms of the quarkonium mass M and temperature T (for $M \gg T$). The ratio $r[\Upsilon(nS)]$ of the yield of different excited bottomonium states to that of ground state is then constructed and contrasted with the available data. Assuming all the resonances in a given quarkonium family are freezing out together inside a fireball of nearly unit fugacity, r contains only a single parameter, the freeze-out temperature T_F. Accounting for the modification of primordial densities due to feed-down decay from excited states and neglecting the errors in the branching ratio, the yield ratio of $\Upsilon(2S)$ and $\Upsilon(1S)$ states indicated a preliminary estimation of the chemical freeze-out temperature $T_F = 222^{+28}_{-29}$ MeV, which is much higher than that of light hadrons. One may note that the idea of quark flavor dependent sequential freeze-out of the hadrons measured in relativistic heavy-ion collisions was first argued in Ref. [45]. A systematic analysis of the hadron yields within a thermodynamically consistent hadron resonance gas model at different collision energies indicated the strange hadrons freezing out earlier at a higher temperature than the nonstrange light hadrons. Reference [40] was the first extension of this two chemical freeze-out (CFO) picture to the charm and bottom sector and thus advocating for a multi-CFO scenario in heavy ion collisions at LHC. The extracted T_F was found to be roughly unchanged with the collision centrality, with a tendency of a very mild drop towards most central collisions indicating a slight earlier freeze-out in peripheral collisions or a weak contamination by spectator nucleons. The near constancy of T_F across various centrality bins was considered as evidence for thermalization, in a sense that initial state information is forgotten.

These results, however, suffered from the large uncertainty associated with the then available data, forbidding one to make any mature claim. Analysis of the then available preliminary charmonium data from the CMS Collaboration, in the same model framework, after removing the nonprompt contribution from b-hadron decays gives $T_f = 159 \pm 31$ MeV at central rapidity and 265 ± 59 MeV at forward rapidity. The significant difference in T_f at the two rapidity intervals is attributed to the different p_T acceptance of the corresponding data samples. Higher p_T charmonia are likely to escape more easily from the fireball and thus have lesser probability of undergoing complete thermalization. Smaller T_F for larger p_T threshold thus indicates that charmonia which are sampled are yet to be equilibrated with the fireball. Decreasing T_F towards more peripheral collisions, in both forward and central rapidity intervals, lends support to this interpretation. The unavailability of suitable low-p_T charmonia data samples prevented any robust determination of their freeze-out temperature. Compared to then, the situation is much improved now in terms of availability of high precision data. Both CMS and ALICE Collaborations have collected high statistics data for quarkonium production in p-p, p-Pb, and Pb-Pb collisions.

This motivates us to perform a reinvestigation of quarkonia chemical freeze-out analysis at LHC, by investigating their relative production yields in nuclear collisions. In this article, we have employed a semiclassical grand canonical approach and analyzed the relative yields of different bottomonia and

charmonia states produced in Pb-Pb, p-Pb, and high multiplicity p-p collisions at LHC. We have also systematically investigated the dependence of chemical freeze-out temperature on the collision centrality. The article is organized in the following way. Section II gives a brief introduction to the statistical model used in our calculation. The analysis of quarkonium yield ratios for different collision systems and at different energies within our model framework is performed in Sec. III. The main results of our investigation are summarized in Sec. IV.

II. BRIEF DESCRIPTION OF THE MODEL

The model used here is a thermal statistical model based on the semiclassical grand canonical approach. The model is similar to the famous hadron resonance gas (HRG) model that has been very successful in describing the particle abundances and thereby extracting the thermodynamic parameters of the fireball at chemical freeze-out [46–51]. The partition function is constructed considering a grand canonical ensemble of noninteracting system of particles obeying quantum statistics. In this model, the primordial yield (N^p) of the ith hadron at zero chemical potential ($\mu = 0$) can be obtained from the following equation [52,53]:

$$N_i^p = \frac{g_i V}{(2\pi)^3} \int d^3\mathbf{p} \frac{1}{\exp\left(\frac{1}{T}\sqrt{m_i^2 + \mathbf{p}^2}\right) \pm 1} \quad (1)$$

where the signs $\pm$ correspond to the fermion and boson respectively and other symbols have their usual meaning.

The measured yield of ith hadron also contains the contribution of decay feed-down from heavier resonances. So, the total multiplicity of the ith hadron is given by the sum of the primordial (N^p) yield as well as the feed-down contribution from heavier resonance states, i.e.,

$$N_i^t = N_i^p + \sum_j N_j^p \times \mathrm{BR}_{j \to i} \quad (2)$$

where $\mathrm{BR}_{j \to i}$ is the branching ratio of the respective decay channel. We have taken all the quarkonium resonance states and the different branching ratios as available in [54]. Note that we are concerned about the quarkonium states only and therefore all the hadronic states of mass below quarkonium do not contribute to the present calculation.

Another important point of consideration is that experiments do not cover the entire phase space and are rather restricted by different detector acceptance and other experimental constraints. These restrictions result in limited p_T and η coverage of the detectors. Hence, for a realistic comparison between the theoretical model estimation with experimental results, it is imperative to implement kinematic cuts in the model calculation. To incorporate experimental acceptance effects, we express Eq. (1) as [55,56]

$$N_i^p = \frac{g_i V}{4\pi^2} \int d\eta \, dp_T \frac{p_T^2 \cosh\eta}{\exp\left[\frac{1}{T}\sqrt{p_T^2 \cosh^2\eta + m_i^2}\right] \pm 1}, \quad (3)$$

where the limits of the integration, $\eta_{\min} \leqslant \eta \leqslant \eta_{\max}$ and $p_T^{\min} \leqslant p_T \leqslant p_T^{\max}$, are determined from experimental

TABLE I. Summary of the analyzed quarkonia data corpus for heavy-ion collisions, from different experiments at SPS, RHIC, and LHC, along with their kinematic coverage. The freeze-out temperatures are extracted from the excited-to-ground state yield ratios. All the $\sqrt{s_{NN}}$ and p_T are in TeV and GeV/c units, receptively.

System	$\sqrt{s_{NN}}$	Expt.	Ref.	Kinematic acceptance
			Bottomonium	
Au-Au	0.2	STAR	[63]	$p_T < 10, |y| < 1.0$
Pb-Pb	2.76	CMS	[25,57]	$p_T > 0, |y| < 2.4$
Pb-Pb	5.02	CMS	[59,60,62]	$p_T < 30, |y| < 2.4$
Pb-Pb	5.02	ALICE	[58]	$p_T < 15, 2.5 < y < 4$
Pb-Pb	5.02	ATLAS	[61]	$p_T < 30, |y| < 1.5$
			Charmonium	
Pb-Pb	0.017	NA50	[65]	$p_T > 0, 0 < |y| < 1$
Pb-Pb	2.76	CMS	[66,67]	$3 < p_T < 30, 1.6 < y < 2.4$
				$6.5 < p_T < 15, |y| < 1.6$
Pb-Pb	2.76	ALICE	[17]	$p_T < 15, 2.5 < |y| < 4$
Pb-Pb	5.02	CMS	[22,23]	$3 < p_T < 30, |y| < 1.6$
Pb-Pb	5.02	ALICE	[22–24]	$p_T < 12, 2.5 < |y| < 4$

kinematic cuts. Unless explicitly mentioned, these kinematic cuts are implemented in all of the analyses.

III. ANALYSIS RESULTS

In this section, we separately study relative quarkonium yields in heavy ion collisions and in small systems (p-p and p-A collisions) at LHC.

A. A-A system

We begin with the thermal analysis of the relative quarkonium yields in Pb-Pb collisions at LHC. The data sets for various quarkonium states used in our analysis are summarized in Table I and correspond to $J/\psi(1S)$ and $\psi(2S)$ states in the charmonia sector and $\Upsilon(1S)$, $\Upsilon(2S)$ and $\Upsilon(3S)$ states in the bottomonia sector, all reconstructed via their dimuon ($\mu^+\mu^-$) decay channel. In addition to the available LHC data, recently published STAR data on bottomonium production in $\sqrt{s_{NN}} = 200$ GeV Au-Au collisions at RHIC and the available ψ-to-J/ψ ratio in $\sqrt{s_{NN}} = 17.3$ GeV Pb-Pb collisions measured by the NA50 Collaboration at SPS are also examined for completeness. For a consistency check, it is imperative to compare our model analysis with the previously obtained results [40].

We thus start by reporting our results of Υ production at midrapidity, measured by the CMS collaboration, in $\sqrt{s_{NN}} = 2.76$ TeV Pb-Pb collisions [25,57]. As previously argued, R_{AA} and the double ratio are not useful quantities to perform a thermal analysis of the heavy mesons produced in these collisions. Instead, to extract thermal parameters, like freeze-out temperature employing the thermal model, one needs a single ratio $r_{PbPb}[h_2] = N_{PbPb}[h_2]/N_{PbPb}[h_1]$, i.e., relative yields of different hadronic states produced in the same collision system. We have used the Pb-Pb single ratios of different bottomonium states, $r_{PbPb}[\Upsilon(2S)] = N_{PbPb}[\Upsilon(2S)]/N_{PbPb}[\Upsilon(1S)]$, as reported in [57] to extract the centrality dependence of freeze-out temperature, T_f. The results of our analysis are

TABLE II. The freeze-out temperature of the bottomonium states produced in $\sqrt{s_{NN}} = 200$ GeV Au-Au collisions as measured by the STAR Collaboration at RHIC and in $\sqrt{s_{NN}} = 2.76$ TeV and 5.02 TeV Pb-Pb collisions at LHC as measured by ALICE, CMS, and ATLAS Collaborations at LHC. All the temperatures and $\sqrt{s_{NN}}$ are in MeV and TeV units respectively. "WOAC" and "WAC" represent without and with acceptance correction, respectively.

$\sqrt{s_{NN}}$	$\langle N_{\mathrm{part}}\rangle$	Collaboration	T_f(WOAC)	T_f(WAC)
			Bottomonium	
	Kinematic range: $p_T < 10$ GeV/c, $|y| < 1.0$			
0.20	88	STAR	371.35^{+117}_{-92}	371.35^{+117}_{-92}
0.20	210	STAR	342.16^{+116}_{-93}	342.16^{+116}_{-93}
0.20	335	STAR	196.75^{+86}_{-177}	196.75^{+86}_{-177}
0.20	CI (0–60%)	STAR	288.43^{+53}_{-49}	288.43^{+53}_{-49}
	Kinematic range: $p_T > 0$ GeV/c, $|y| < 2.4$			
2.76	22	CMS	249.70^{+71}_{-73}	249.70^{+71}_{-73}
2.76	86	CMS	298.56^{+110}_{-96}	298.56^{+110}_{-96}
2.76	130	CMS	259.34^{+63}_{62}	259.34^{+63}_{62}
2.76	187	CMS	288.59^{+61}_{-56}	288.59^{+61}_{-56}
2.76	261	CMS	178.96^{+51}_{-178}	178.96^{+51}_{-178}
2.76	329	CMS	167.12^{+62}_{-167}	167.12^{+62}_{-167}
2.76	381	CMS	230.27^{+61}_{-67}	230.27^{+61}_{-67}
2.76	CI (0–100%)	CMS	221^{+26}_{-27}	221^{+26}_{-27}
	Kinematic range: $p_T < 30$ GeV/c, $|y| < 2.4$			
5.02	8.3	CMS	399.26^{+208}_{-138}	399.26^{+208}_{-138}
5.02	30.6	CMS	299.13^{+68}_{-61}	299.13^{+68}_{-61}
5.02	53.9	CMS	243.66^{+56}_{-57}	243.66^{+56}_{-57}
5.02	87.0	CMS	272.72^{+51}_{-49}	272.72^{+51}_{-49}
5.02	131.4	CMS	259.76^{+40}_{-39}	259.76^{+40}_{-39}
5.02	189.2	CMS	262.10^{+40}_{39}	262.10^{+40}_{39}
5.02	264.2	CMS	230.73^{+42}_{-44}	230.73^{+42}_{-44}
5.02	333.3	CMS	256.54^{+53}_{-53}	256.54^{+53}_{-54}
5.02	384.3	CMS	<250.10	<250.10
5.02	CI (0–100%)	CMS	235^{+19}_{-20}	235^{+19}_{-20}
	Kinematic range: $p_T < 15$ GeV/c, $2.5 < y < 4$			
5.02	54.3	ALICE	293.625^{+47}_{-44}	293.625^{+47}_{-44}
5.02	269.1	ALICE	230.435^{+31}_{-32}	230.435^{+31}_{-32}
	Kinematic range: $p_T < 30$ GeV/c, $|y| < 1.5$			
5.02	46.5	ATLAS	322.15^{+55}_{-52}	322.15^{+55}_{-52}
5.02	160.496	ATLAS	244.44^{+49}_{-50}	244.44^{+49}_{-50}
5.02	264.62	ATLAS	215.12^{+47}_{-55}	215.12^{+48}_{-55}
5.02	362.98	ATLAS	<212.75	<212.76
5.02	CI (0–80%)	ATLAS	253.53^{+45}_{-45}	253.53^{+46}_{-45}

listed in Table II and displayed in the upper panel of Fig. 1. Our estimated value of T_f, extracted from the centrality integrated relative yield, comes out to be 221^{+21}_{-22} MeV, in close agreement with the previous result. Also, as found earlier, no strong centrality dependence of T_f is observed, apart from a mild drop towards more central collisions. The errors in the extracted T_f values are estimated from calculations with
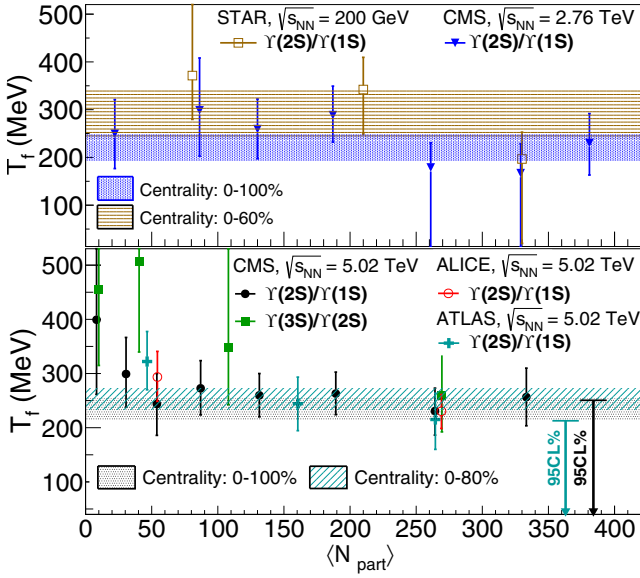
FIG. 1. The centrality dependence of the freeze-out temperature (T_f) of the Υ mesons, in the A-A collision systems, extracted using different relative yields of the bottomonium states measured by different ultrarelativistic heavy ion experiments. Upper panel: T_f extracted from data collected by the CMS Collaboration at LHC in $\sqrt{s_{NN}} = 2.76$ TeV Pb-Pb collisions and by the STAR Collaboration at RHIC in $\sqrt{s_{NN}} = 200$ GeV Au-Au collisions. Lower panel: T_f is extracted from the data collected by CMS, ALICE, and ATLAS Collaborations in $\sqrt{s_{NN}} = 5.02$ TeV Pb-Pb collisions. The band for both panels represents T_f for centrality integrated events. The references and kinematic acceptance of the corresponding experimental data are given in Table I.

the bottomonia yields varied between given errors. The most recent measurements of Υ production in $\sqrt{s_{NN}} = 2.76$ TeV Pb-Pb collisions by the CMS Collaboration is reported in Ref. [30], in the same kinematic domain but with improved statistics and precision compared to their previous run [25]. In line with previous measurements, a strong centrality-dependent suppression is observed in Pb-Pb relative to p-p collisions, by factors of up to approximately 2 and 8, for the $\Upsilon(1S)$ and $\Upsilon(2S)$ states, respectively. The corresponding T_f extracted from the centrality integrated yield ratios comes out to be 201^{+21}_{-23} MeV. A centrality differential measurement is, however, not possible due to the difference in the published centrality bins for the $\Upsilon(1S)$ and $\Upsilon(2S)$ states.

The measurement of Υ production at $\sqrt{s_{NN}} = 5.02$ TeV Pb-Pb collisions is now made available by CMS, ALICE, and ATLAS Collaborations at LHC. While $r_{PbPb}[\Upsilon(2S)]$ is directly available from ALICE [58], CMS and ATLAS do not provide the single ratio, rather they present their results in terms of double ratios [59–61]. Hence, in order to construct the corresponding $r_{PbPb}[\Upsilon(2S)]$ from CMS and ATLAS data sets, we multiply the double ratio with the pp single ratio, $r_{pp}[\Upsilon(2S)]$, which is obtained by integrating the differential cross sections as a function of rapidity and p_T given in [62] and [61] by CMS and ATLAS Collaborations respectively. The corresponding T_f values extracted for various collision centralities are displayed in the lower panel of Fig. 1. The

uncertainty in the estimated T_f is reduced for $\sqrt{s_{NN}} = 5.02$ TeV compared to 2.76 TeV and it is more prominent for more central collisions. No significant collision energy dependence in T_f has been observed and the overall trend, namely the centrality independence and modest decrease of freeze-out temperature for the most central collisions, remains the same for all analyzed data sets as well.

We note that the centrality integrated T_f value as obtained from the ATLAS data set is slightly higher than that extracted from ALICE and CMS. However the integrated data samples available from ATLAS correspond to 0–80% centrality whereas other two experiments published their results for 0–100% collision centrality. It is also interesting to note that the ALICE Collaboration performed measurements at the forward rapidity region ($2.5 < y < 4$), whereas the CMS ($|y| < 2.4$) and ATLAS ($|y| < 1.5$) experiments collected data at midrapidity. However, the corresponding T_f values from ALICE data agree within uncertainty to those extracted from CMS and ATLAS midrapidity data, indicating the near rapidity independence of the freeze-out temperature. This is possibly a direct consequence of boost invariance of the produced fireball at such high collision energy.

Moreover, the CMS Collaboration has also reported the double ratio of excited states, $\Upsilon(3S)/\Upsilon(2S)$, in 5.02 TeV Pb-Pb collisions. We have also utilized this piece of information to extract the corresponding T_f. The number of data points is smaller and associated error bars are larger due to reduced statistics. However, it is conspicuous from the lower panel of Fig. 1 that, although T_f extracted from yield ratios of different states are different at low multiplicity regions, they match within errors at the high multiplicity region, pointing towards a single freeze-out scenario of all bottomonium states in central Pb-Pb collisions. It is also very interesting to note that the application of the detector acceptance cut does not have any effect on the resulting T_f values of the analyzed bottomonia states. All the collaborations have collected the Υ data samples down to $p_T = 0$, though the upper limit of p_T is different. This presumably means that the thermalization of these heavy resonances is dominated by the low momentum states, which spend more time inside the fireball.

For an explicit verification of this fact, we set different upper limits of p_T in our model [see Eq. (3)] and found that the upper limit of p_T beyond 3.5 GeV does not influence the resulting T_f. We finish this discussion with the preliminary analysis of the results on Υ production in $\sqrt{s_{NN}} = 200$ GeV Au-Au collisions at midrapidity, recently made available by the STAR Collaboration at RHIC [63]. Instead of directly providing $r_{AuAu}[\Upsilon(2S)]$, data are published in terms of separate centrality dependence of R_{AA} for 1S and 2S states. Hence to construct the desired single ratio, $R_{AA}[\Upsilon(2S)]$ is first divided by $R_{AA}[\Upsilon(1S)]$ to get the double ratio, and then the single ratio is obtained by multiplying the pp single ratio given in Ref. [64]. The results are included in the upper panel of Fig. 1. Although for central collisions the corresponding T_f values are in close agreement at $\sqrt{s_{NN}} = 200$ GeV and $\sqrt{s_{NN}} = 2.76$ TeV, the centrality integrated value for 0–60% STAR data is larger than that for 0–100% ALICE data.

Let us now turn to the available data in the charmonium sector at LHC. $R_{PbPb}(J/\psi)$ and its systematics have

been reported by the ALICE, ATLAS, and CMS Collaborations. However, the comparison of $\psi(2S)$ and J/ψ is not yet available from ATLAS. For the present study, we have thus analyzed the data from both CMS and ALICE Collaborations at $\sqrt{s_{NN}} = 2.76$ TeV [17,66,67] and $\sqrt{s_{NN}} = 5.02$ TeV [22,24]. The relative yield of ψ' with respect to J/ψ is used to estimate the corresponding T_f. But such extraction should be performed on the prompt charmonium states free from the feed-down contribution from b quark decays. The CMS Collaboration, thanks to their excellent vertex resolution capabilities, has published the prompt yield of J/ψ and ψ' mesons in Pb-Pb collisions. Like bottomonium measurements, CMS primarily provides double ratios in both 2.76 [66] and 5.02 TeV [23] Pb-Pb collisions, except for the centrality integrated single ratio at 2.76 TeV, reported in [67]. Hence, we need to the use pp p_T-differential cross section for prompt $\psi(2S)$ [68] and J/ψ [23] mesons to calculate the p_T-integrated pp single ratio. Subsequently we calculate the prompt Pb-Pb single ratio, $r_{\text{PbPb}}[\psi(2S)] = N_{\text{PbPb}}[\psi(2S)]/N_{\text{PbPb}}[J/\psi]$. The ALICE Collaboration, on the other hand, does not report prompt yields of different charmonium states, but rather provides inclusive yield ratios.

For exclusion of the nonprompt contribution and to construct $r_{\text{prompt}}[\psi(2s)]$ from the ALICE data, we follow the same prescription given in Ref. [40],

$$r_{\text{prompt}}[\psi(2S)] = r[\psi(2S)]\left(\frac{1 - af_B}{1 - f_B}\right). \tag{4}$$

where f_B and af_B are respectively the fraction of J/ψ and $\psi(2S)$ coming from weak decay of B hadrons. f_B is experimentally measured in p-p collisions. The anticipated value of a is based on the ratio of partial widths of the decays $B^+ \rightarrow \psi(2S)\pi$ and $B^+ \rightarrow J/\psi\pi$. In our calculation, we take a central value ≈ 0.5 and vary it from 0 to 1 that contributes to the uncertainty in estimated prompt ratio. At $\sqrt{s_{NN}} = 2.76$ TeV, in the forward rapidity regime, f_B is found to be $10.7 \pm 4.8 \pm 2.5\%$, in the kinematic range $1.5 < p_T < 4.5$ [69]. ALICE recently measured the nonprompt contribution of J/ψ down to $p_T = 1$ GeV at $\sqrt{s_{NN}} = 5.02$ TeV [70]. It appeared that f_B has a strong p_T dependence. In the p_T range of our interest ($p_T < 12$ GeV), f_B varies from 10% to 30% [70]. We take the mean value, i.e., 20% in our calculation. The resulting variation in the T_f is $\approx 7.5\%$ due to the variation in f_B from 10% to 30%, which is added to the uncertainty of the prompt ratio in our analysis. The centrality [69] and rapidity [23] independence of f_B has been considered throughout the analyses. For completeness, we have also analyzed the data available from the NA50 Collaboration at SPS on ψ'-to-J/ψ ratio in $\sqrt{s_{NN}} = 17.36$ GeV Pb-Pb collisions [65]. However, the weak decay contribution is ignored due to negligible production of beauty hadrons at SPS.

The analysis results are displayed in Fig. 2 and tabulated in Table III. For a quantitative comparison, we have calculated T_f both with and without experimental acceptance cuts. One may immediately note the difference between the T_f values extracted from the CMS and ALICE data sets.

For the CMS data corpus, which has a finite low-p_T cutoff, we observe that the acceptance correction significantly reduces the corresponding T_f values at both collision energies.

TABLE III. Same as Table II but for charmonium states.

$\sqrt{s_{NN}}$	$\langle N_{\text{part}}\rangle$	Collaboration	T_f(WOAC)	T_f(WAC)
		Charmonium		
	Kinematic range: $p_T > 0$ GeV/c, $0 < \|y\| < 1$			
0.017	43.72	NA50	190.48^{+19}_{-19}	190.48^{+19}_{-19}
0.017	96.18	NA50	182.15^{+19}_{-19}	182.15^{+19}_{-19}
0.017	146.65	NA50	177.50^{+18}_{-18}	177.50^{+18}_{-18}
0.017	196.86	NA50	167.60^{+17}_{-17}	167.61^{+17}_{-17}
0.017	248.33	NA50	163.98^{+16}_{-17}	163.98^{+16}_{-17}
0.017	298.54	NA50	169.67^{+18}_{-18}	169.68^{+18}_{-18}
0.017	351.89	NA50	159.37^{+17}_{-17}	159.37^{+17}_{-17}
	Kinematic range: $3 < p_T < 30$ GeV/c, $1.6 < \|y\| < 2.4$			
2.76	32.8	CMS	174.40^{+24}_{-27}	82.06^{+13}_{-14}
2.76	158.6	CMS	177.20^{+31}_{-36}	83.95^{+15}_{-18}
2.76	308.4	CMS	251.27^{+35}_{-33}	126.05^{+15}_{-14}
2.76	CI	CMS	220.10^{+17}_{-17}	105.41^{+9}_{-9}
	Kinematic range: $6.5 < p_T < 30$ GeV/c, $\|y\| < 1.6$			
2.76	32.8	CMS	<153.33	<78.72
2.76	158.6	CMS	170.11^{+8}_{-8}	87.41^{+5}_{-5}
2.76	308.4	CMS	156.55^{+13}_{-15}	80.09^{+6}_{-7}
2.76	CI	CMS	151.69^{+9}_{-8}	77.75^{+6}_{-5}
	Kinematic range: $p_T < 15$ GeV/c, $2.5 < y < 4$			
2.76	17.51	ALICE	160.59^{+19}_{-22}	160.60^{+19}_{-22}
2.76	68.6	ALICE	130.57^{+24}_{-52}	130.58^{+24}_{-52}
2.76	157.2	ALICE	139.17^{+19}_{-26}	139.18^{+19}_{-26}
2.76	308.1	ALICE	<128.20	<128.32
	Kinematic range: $6.5 < p_T < 30$ GeV/c, $\|y\| < 1.6$			
5.02	22	CMS	194.54^{+17}_{-19}	98.78^{+9}_{-10}
5.02	87	CMS	172.98^{+15}_{-16}	86.35^{+7}_{-8}
5.02	131	CMS	211.31^{+10}_{-10}	106.78^{+6}_{-6}
5.02	189	CMS	211.83^{+13}_{-13}	107.05^{+7}_{-7}
5.02	264	CMS	179.98^{+15}_{-16}	90.05^{+8}_{-8}
5.02	359	CMS	<214.43	<109.57
5.02	CI	CMS	182.72^{+15}_{-16}	91.50^{+9}_{-9}
	Kinematic range: $p_T < 12$ GeV/c, $2.5 < y < 4$			
5.02	17	ALICE	242.25^{+56}_{-45}	214.46^{+50}_{-40}
5.02	70	ALICE	239.14^{+48}_{-38}	211.38^{+43}_{-34}
5.02	159	ALICE	228.81^{+46}_{-38}	228.81^{+45}_{-38}
5.02	308	ALICE	249.86^{+55}_{-43}	249.86^{+55}_{-43}

CMS measured charmonium production at $\sqrt{s_{NN}} = 2.76$ TeV in forward ($1.5 < |y| < 2.4$) and midrapidity ($|y| < 1.6$) regions with p_T coverages of $3 < p_T < 30$ GeV/c and $6.5 < p_T < 30$ GeV/c, respectively, and at $\sqrt{s_{NN}} = 5.02$ TeV only in the midrapidity region where the p_T coverage is same as that of the previous one. For midrapidity (larger p_T threshold) the corresponding T_f values are smaller than those at forward rapidity. For a given low-p_T threshold, T_f increases for more central collisions. These observations are in line with previous findings where it was attributed to different p_T acceptances. The selected high-p_T mesons would spend less time inside
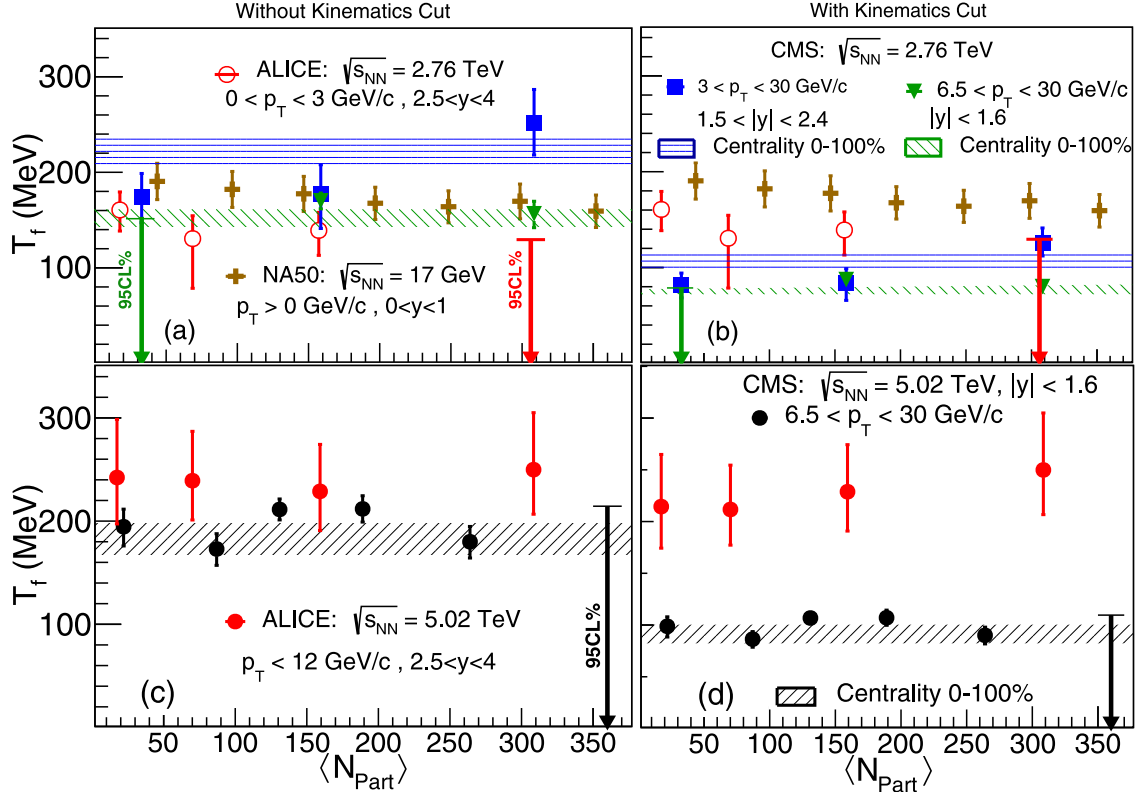
FIG. 2. The centrality dependence of freeze-out temperature for charmonia states without (left) and with (right) the acceptance correction effect, extracted using $r_{prompt}[\psi(2S)]$, in the Pb-Pb collisions at $\sqrt{s_{NN}} = 2.76$ and 5.02 TeV measured by ALICE and CMS Collaborations at LHC. For completeness, T_f values estimated in $\sqrt{s_{NN}} = 17.3$ GeV Pb-Pb collisions, as measured by NA50 Collaboration at SPS, are also shown. The band represents T_F for centrality integrated events. The red bands corresponding to ALICE 2.76 TeV and ALICE 5.02 TeV are absent due to to the unavailability of corresponding data for centrality integrated yields from the ALICE Collaboration.

the medium and thus are less likely to be thermalized with the fireball. Note that in the previous work the acceptance effect was not taken into account. Explicit incorporation of the finite acceptance correction in our calculations and resulting reduction in the freeze-out temperature directly manifests the effect of the large minimum p_T threshold of the analyzed charmonia data sets. A thermal interpretation of the charmonium data sampled by the CMS Collaboration is thus possibly incorrect. One may take note of the fact that the recent measurements by the CMS Collaboration of J/ψ production inside jets in $\sqrt{s} = 8$ TeV p-p collisions led them to conclude jet fragmentation as the dominant source of high-p_T ($E_{J/\psi} > 15$ GeV) prompt J/ψ at midrapidity [71].

This claim gets further support from the analysis of now available ALICE data. For the ALICE data sample, measured at forward rapidity ($2.5 < y < 4.0$), the minimum threshold value of p_T is as low as zero and the effect of acceptance correction on the resulting T_f is absent. These data points thus give a genuine T_f of the charmonium system at LHC. For most central collisions, the T_f for charmonium states in 2.76 TeV Pb-Pb collisions comes out to be around 140 MeV. Accounting for the related uncertainty, the value is in agreement with the freeze-out temperature of light hadrons. At 5.02 TeV the corresponding value of T_f is around 250 MeV. Contrary to the CMS results, a mild drop in T_f is observed

with increasing collision centrality. The large recombination effect in the charmonium sector [73,74] may explain the high value of T_f extracted from ALICE 5.02 TeV data [24]. As shown in Ref. [24], the centrality dependence ratio is well explained by a model such as TAMU (Texas A&M University) [75] that takes recombination into account during the plasma phase. The effect of recombination is found to be stronger for $\psi(2S)$ than J/ψ, leading to larger values of the yield ratio and hence the corresponding T_f. For the two most peripheral bins of ALICE data at 5.02 TeV, we observe a sensitivity in the T_f values to the detector acceptance. A low-p_T cutoff of 300 MeV was set in the analyzed data for these two peripheral bins to get rid of the charm contribution from photoproduction [24], which then affects the resulting T_f values.

Before we move on, it will also be interesting to investigate the available data on transverse momentum (p_T) spectra of J/ψ mesons in Pb-Pb collisions at LHC, following the thermal model description of Eq. (3). This would be an additional validation of our thermal model description with finite phase space coverage. However one needs to keep in mind that the particle multiplicities or their ratios probe the chemical freeze-out temperature (T_f), while the p_T spectra probe the kinetic freeze-out temperature (T_{kin}). Also the effect of medium expansion is folded in the inverse slope parameter of the p_T spectra and hence boosted thermal models such as
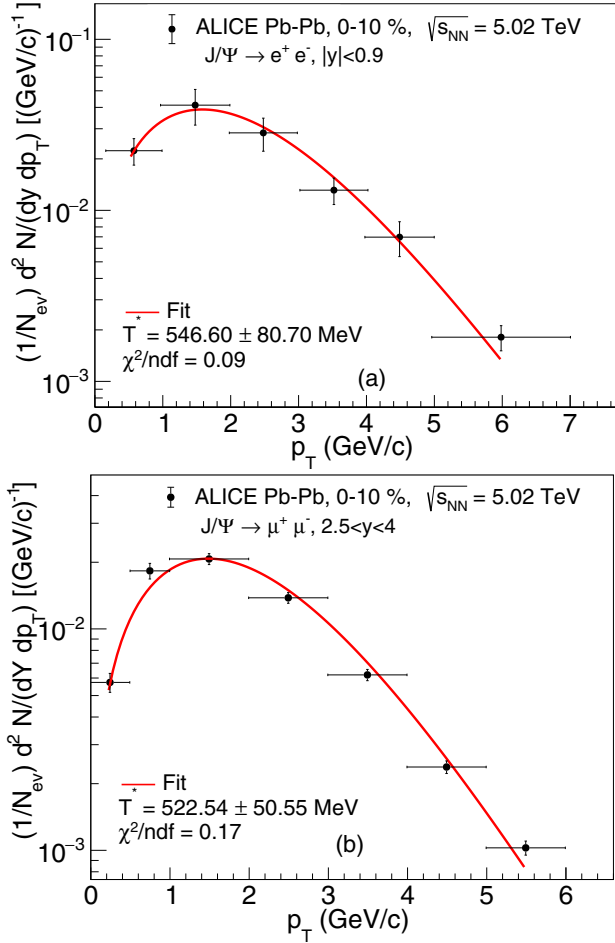
FIG. 3. Thermal model fits to the transverse momentum (p_T) spectra of J/ψ mesons in $\sqrt{s_{NN}} = 5.02$ TeV most central (0–10%) Pb-Pb collisions at (a) midrapidity ($|y| < 0.9$) [72] and (b) forward rapidity ($2.5 < y < 4.0$) [20]. The fits are restricted up to $p_T \approx 6$ GeV/c. For both the data sets the fit qualities are similar (comparable values of χ^2 per degree of freedom (χ^2/ndf) and the corresponding effective temperature (T^*) values match within errors.

blast wave models are more suitable to analyze thermal distributions. Nevertheless we have tried to fit the p_T distribution of the J/ψ mesons in 5.02 TeV most central Pb-Pb collisions at LHC, measured by ALICE Collaboration, both at midrapidity ($|y| < 0.9$) and at forward rapidity ($2.5 < y < 4.0$), using Eq. (3). We restrict our fit up to p_T of 6 GeV/c in order to remove other effects like "corona" contribution and jet fragmentation [29]. The fit results are displayed in Fig. 3. We obtain the so-called effective temperatures $T^* = 546.60 \pm 80.70$ MeV at midrapidity and $T^* = 522.54 \pm 50.55$ MeV at forward rapidity. The extracted T^* values match within errors. The corresponding kinetic freeze-out temperatures can be obtained from the approximate relation $T^* \simeq T_{\mathrm{kin}} + 1/2 m_{J/\psi} \beta^2$ [76], where β denotes the average transverse velocity of the fireball. For heavy mesons like J/ψ, we assume $T_{\mathrm{kin}} \simeq T_f \simeq 250$ MeV, as obtained in Table III. We get mean transverse velocity $\beta = 0.44$ at midrapidity and $\beta = 0.42$ at forward rapidity, which are reasonable estimates.

TABLE IV. Same as Table I, but for the p-p and p-Pb systems.

System	$\sqrt{s_{NN}}$	Expt.	Ref.	Kinematic acceptance
Small systems: p-p, p-Pb				
Bottomonium				
p-p	2.76	CMS	[57]	$p_T > 0$ GeV/c, $|y| < 1.93$
p-p	7	CMS	[77]	$p_T > 0$ GeV/c, $|y| < 1.93$
p-p	13	ALICE	[78]	$p_T > 0$ GeV/c, $2.5 < y < 4$
p-Pb	5.02	CMS	[57]	$p_T > 0$ GeV/c, $|y| < 1.93$
p-Pb	8.16	ALICE	[79]	$p_T < 15$ GeV/c
Charmonium				
p-p	5.02	ALICE	[80]	$0 < p_T < 12$
p-p	7	ALICE	[81]	$0 < p_T < 12$
p-p	8	ALICE	[82]	$0 < p_T < 12$
p-p	13	ALICE	[83]	$0 < p_T < 16$
p-Pb	w5.02	ALICE	[84]	$-4.46 < y < -2.96$, $2.03 < y < 3.53$, $p_T < 20$ GeV/c
p-Pb	5.02	ALICE	[85]	$p_T < 8$ GeV/c
p-Pb	8.16	ALICE	[86]	$-4.46 < y < -2.96$, $2.03 < y < 3.53$, $p_T < 20$ GeV/c
p-Pb	8.16	ALICE	[87]	$p_T < 20$ GeV/c

B. Small systems (p-p, p-Pb)

Recently, some of the collective features of heavy ion collisions were also observed in the systems formed in pp and p-Pb collisions, contradicting the traditional wisdom. Some experimental findings that triggered the debate on the origin of the collectivity in small systems are long-range, near-side azimuthal correlation [88–91], mass-ordering of elliptical flow [92], and p_T-dependent v_2 [93], among others. In view of this situation, it is interesting to test the thermal behavior of the quarkonium states produced in the p-p and p-Pb collisions with that of heavy ion collisions.

The analyzed data corpora as available from CMS and ALICE Collaborations are summarized in Table IV. We begin with the analysis of the relative yields of bottomonia measured at different collision energies and for the p-p and p-Pb collision systems. For both collision systems, we have extracted T_f for different track multiplicity classes (mimicking collision centrality) using both the ratios $r_{pp(Pb)}(\Upsilon(2S))$ and $r_{pp(Pb)}(\Upsilon(3S))$. The results are shown in Fig. 4. The upper panel shows the multiplicity-dependent freeze-out temperatures in the p-p collisions, extracted using the CMS data samples collected at $\sqrt{s_{NN}} = 2.76$ TeV [57], $\sqrt{s_{NN}} = 7$ TeV [77], and also ALICE data at $\sqrt{s_{NN}} = 13$ TeV [78]. Note that CMS presents their results in terms of average N_{track}, whereas ALICE prefers to use corrected tracklets, $N_{\mathrm{trk}}^{\mathrm{cor}}$. The T_f extracted from both types of relative yields has not shown any significant $\sqrt{s}$ dependence, though there is a tendency of decreasing T_f, extracted from minimum bias events, with increasing $\sqrt{s}$.

Note that, similarly to the Pb-Pb collision system, there is an indication of lowering of the T_f for higher multiplicity events, though the value of T_f for the high multiplicity class is almost 1.7 times larger than the T_f we obtained for the centrality integrated Pb-Pb system. The most intriguing feature that
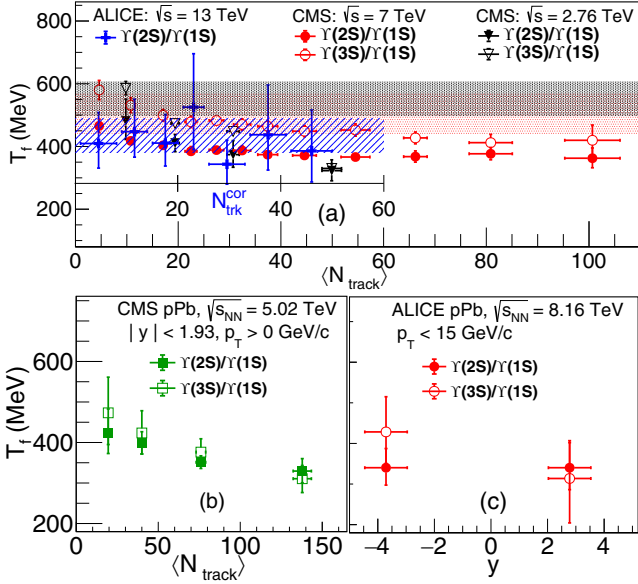
FIG. 4. (a) Upper panel: The track multiplicity dependence of the bottomonia freeze-out temperature for the p-p collision systems at $\sqrt{s_{NN}} = 2.76$, 7, and 13 TeV. The band represents T_f for minimum bias events. (b) Lower left panel: Same as the upper panel but for the p-Pb collisions at $\sqrt{s_{NN}} = 5.02$ TeV. (c) Lower right panel: Bottomonia freeze-out temperature as a function of rapidity for p-Pb collisions at $\sqrt{s_{NN}} = 8.16$ TeV. The freeze-out temperatures are extracted using the relative yields of the different bottomonium states. The references and kinematic acceptance of the corresponding experimental data are given in the Table IV (see text for details).
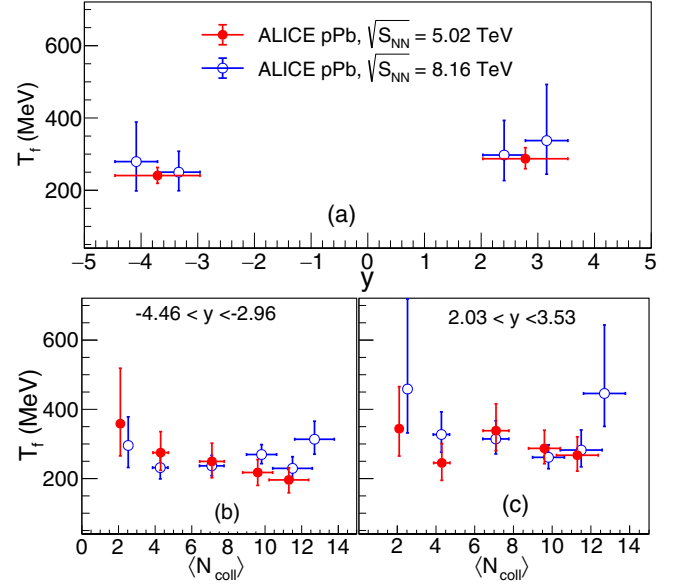

FIG. 5. (a) Upper panel: Rapidity dependence of the charmonia freeze-out temperature in p-Pb collisions at $\sqrt{s_{NN}} = 5.02$ and 8.16 TeV. (b) Lower left panel: Centrality dependence of the charmonia freeze-out temperature in $\sqrt{s_{NN}} = 5.02$ and 8.16 TeV p-Pb collisions at backward hemisphere. The centrality is estimated in terms of the average number of binary collisions ($\langle N_{coll} \rangle$). (c) Lower right panel: Same as (b) but at forward hemisphere. The freeze-out temperatures are extracted using the relative yields of the different charmonium states. The references and kinematic acceptance of the corresponding experimental data are given in Table IV (see text for details).

resembles the feature of the Pb-Pb system is the simultaneous freeze-out of all the states at higher multiplicity events. Our analysis results for the p-Pb system are shown in the lower panel of the Fig. 4. The multiplicity dependence of the T_f for midrapidity CMS data at $\sqrt{s_{NN}} = 5.02$ TeV [57] and the multiplicity integrated rapidity dependence of T_f using ALICE data at $\sqrt{s_{NN}} = 8.16$ TeV [79] are presented in the lower-left and lower-right panels respectively. Like the p-p collision system, lowering of the T_f and simultaneous freeze-out of different bottomonia states with increasing track multiplicity has been observed. One may note that the T_f extracted at the backward rapidity is slightly higher than that of the forward-rapidity region, but it is not completely conclusive because of the large uncertainty. Implementation of finite phase space coverage of the data is not seen to generate any visible effect on the resulting T_f values.

We have also analyzed the relative yields of charmonium states measured in p-Pb collisions at $\sqrt{s_{NN}} = 5.02$ TeV [84] and $\sqrt{s_{NN}} = 8.16$ TeV [86], and also in p-p collisions at $\sqrt{s_{NN}} = 5.02$, 7, 8, 13 TeV as made available by the ALICE Collaboration [80–83]. In this sector also we analyzed the freeze-out temperatures both with and without considering the acceptance correction effect. Moreover, like all previous cases, the experimental p_T range goes down to zero, thus no effect of the acceptance correction has been found. To exclude the nonprompt contribution, the f_B values in the p-Pb system are taken as $12.4 \pm 0.89\%$ at forward rapidity and $8.37 \pm 1.12\%$ at backward rapidity at 5.02 TeV [94]. At 8.16 TeV, the

corresponding contribution is $14.51 \pm 1.06(10.99 \pm 1.1)\%$ in the forward (backward) region [95]. Similarly, in p-p collisions, the f_B values at $\sqrt{s} = 5.02$, 7 and 13 TeV are taken as $15.7 \pm 2.3 \pm 1.5\%$ (measured in the kinematic domain $p_T > 1$ GeV/c, $|y| < 0.9$), 20% (since in the p_T range 0–10 GeV/c f_B varies in the range 10–30%), and $18.5 \pm 1.5 \pm 1.4\%$ respectively as available in [96].

Though the ATLAS Collaboration measured the non-prompt contribution of J/ψ as a function of p_T in the 8 TeV p-p collision, the starting p_T range is as large as 8 GeV [97]. Thus to analyze 8 TeV ALICE data [82] in the p_T coverage, $0 < p_T < 12$, we consider the same variation of f_B in the concerned p_T range as has been found in other $\sqrt{s}$, which are around 10% to 30%. In our analyses the variation of f_B with p_T has accounted accordingly for all the cases. The finding of this analysis for p-Pb and p-p are presented in Figs. 5 and 6 respectively. The freeze-out temperature as a function of collision centrality (expressed in terms of average number of binary collisions) is shown separately for forward (lower right panel) and backward (lower left panel) rapidity regions. No significant collision energy or rapidity dependence of T_f has been observed. Apart from the most central and most peripheral data points (at 8.16 TeV), where the uncertainty is huge, for all other data points in both rapidity intervals there is an overall tendency to decrease in T_f with increasing collision centrality, but this is not so conclusive. As noted earlier, the extracted T_f for all investigated data sets are
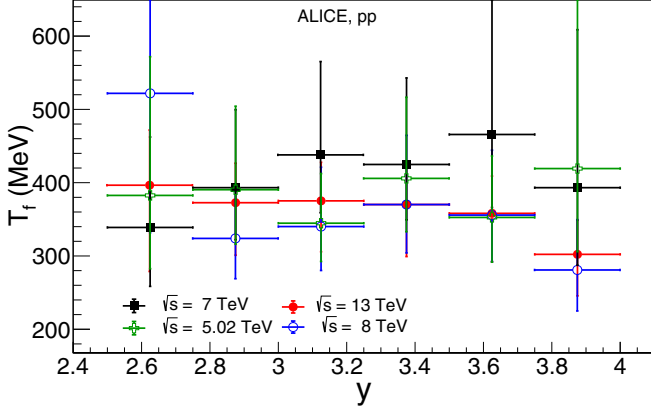
FIG. 6. Rapidity dependence of the charmonium freeze-out temperatures in the forward regions, in *p-p* collisions at different center-of-mass energies ($\sqrt{s}$). The freeze-out temperatures are extracted using the relative yields of the different charmonium states. The references and kinematic acceptance of the corresponding experimental data are given in Table IV (see text for details).

significantly larger than the T_f we obtain from analyzing the relative yield of the Pb-Pb system at 2.76 TeV from ALICE data [see Fig. 2]. The unnaturally high value of quarkonia freeze-out temperature obtained for small collision systems might point towards the fact that the produced quarkonia states are far from thermalized. Alternatively it might also

occur that the lifetime of the produced fireball in these collisions is quite small, leading to the early freeze-out of these quarkonia states.

To further investigate the possibility of quarkonia thermalization in small collision systems at LHC, we adopt the following heuristic. We perform a single parameter (T_f) thermal model fit of the excited [$\Upsilon(2S)$] to ground state [$\Upsilon(1S)$] yield ratio of the bottomonia states for various centrality bins in Pb-Pb and *p-p* collisions. The most peripheral bins are excluded from the analysis. The fit results are displayed in Fig. 7 and summarized in Table V. The resulting fit quality is not very different for Pb-Pb and *p-p* collisions. The χ^2 per degree of freedom (χ^2/ndf) values in the range 1–3 for *p-p* collisions can be attributed to the large error bars associated with the corresponding yield ratio data points. Interestingly the extracted T_f values in the case of Pb-Pb collisions is similar within errors to that obtained from the centrality integrated yield ratio, that plausibly indicates the thermal nature of these heavy hadrons in Pb-Pb collisions. However, for *p-p* collisions the two T_f values (one extracted from the combined fit of yield ratios in different centrality bins and the other calculated from the centrality integrated yield ratio) are largely different. This makes the thermal description of quarkonia in *p-p* collisions questionable. We refrain from performing this exercise for bottomonium production in *p*-Pb collisions due to the small number of reported centrality bins. Similarly, the charmonium sector is difficult as centrality bins are not reported for *p-p* collisions.
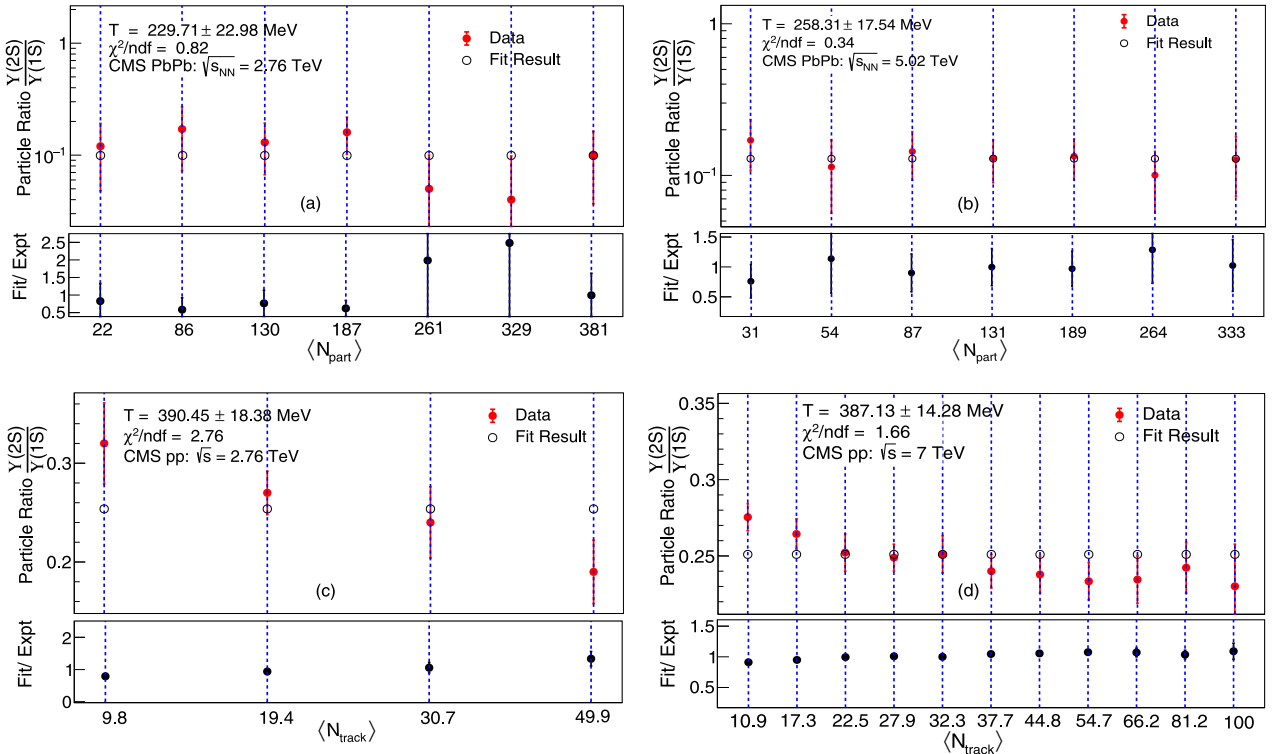

FIG. 7. Single parameter (T_f) thermal model fit to the excited [$\Upsilon(2S)$] to ground state [$\Upsilon(1S)$] ratio of the bottomonia states for various centrality bins in (a) $\sqrt{s_{NN}} = 2.76$ TeV and (b) $\sqrt{s_{NN}} = 5.02$ TeV Pb-Pb and in (c) $\sqrt{s_{NN}} = 2.76$ TeV and (d) $\sqrt{s_{NN}} = 7$ TeV *p-p* collisions. The most peripheral bins are excluded from the analysis. The fit-to-data ratios are also shown for each system.

TABLE V. Results of single parameter (T_f) thermal model fit to the excited [$\Upsilon(2S)$] to ground state [$\Upsilon(1S)$] ratio of the bottomonia for various centrality bins in $\sqrt{s_{NN}} = 2.76$ TeV and $\sqrt{s_{NN}} = 5.02$ TeV Pb-Pb and in $\sqrt{s_{NN}} = 2.76$ TeV and $\sqrt{s_{NN}} = 7$ TeV p-p collisions. The most peripheral bins are excluded from the analysis. Data point for centrality integrated yield ratio in $\sqrt{s_{NN}} = 2.76$ TeV p-p collisions is unavailable.

		Thermal fit results			
System	Collision energy	Yield ratio	χ^2/ndf	T_f(Simultaneous fit of different centrality bin data) (MeV)	T_f(centrality integrated yield ratio) (MeV)
Pb-Pb	2.76 TeV	$\Upsilon(2S)/\Upsilon(1S)$	0.82	229.71 ± 22.98	221.0 ± 26.0
Pb-Pb	5.02 TeV	$\Upsilon(2S)/\Upsilon(1S)$	0.34	258.31 ± 17.54	235.0 ± 19.0
p-p	2.76 TeV	$\Upsilon(2S)/\Upsilon(1S)$	2.76	390.45 ± 18.38	–
p-p	7 TeV	$\Upsilon(2S)/\Upsilon(1S)$	1.66	387.13 ± 14.28	500 ± 59

IV. SUMMARY

In this article, we have analyzed the relative yields of different bottomonia and charmonia states produced in Pb-Pb collisions at LHC, within a thermal statistical model framework. The underlying assumption is the early thermalization and subsequent freeze-out of these heavy hadrons resulting in their chemical freeze-out at temperatures significantly higher than that of light and strange hadrons. All three bottomonium states are seen to be simultaneously frozen in the fireball, at a temperature of around 230 MeV, independent of collision energy. No significant rapidity dependence of T_f has been observed as a possible outcome of boost invariance. The systematic dependence of T_f on the collision centrality is investigated in detail. Insensitivity of the extracted T_f values on the detector phase space coverage possibly indicates the thermalization of the Υ states as measured by different experimental collaborations. In the charmonia sector the data collected by the CMS Collaboration suffer from the presence of a very high value of low-p_T threshold, thus they are unsuitable for any thermal analysis. Analysis of the ALICE data suggests an early thermalization of the charmonia in 5.02 TeV Pb-Pb collisions. Our investigations were also extended to analyze the available quarkonium production in p-Pb and high multiplicity p-p collisions. Although the qualitative patterns of the freeze-out systematics in these small collision systems are similar to those seen in heavy-ion collisions, the T_f values appear to be unrealistically large. Further investigations are necessary to make any robust conclusion about the thermalization of heavy hadrons in small collision systems.

[1] T. Matsui and H. Satz, J/ψ suppression by quark-gluon plasma formation, Phys. Lett. B **178**, 416 (1986).

[2] R. Vogt, J/ψ production and suppression, Phys. Rep. **310**, 197 (1999).

[3] H. Satz, Colour deconfinement and quarkonium binding, J. Phys. G **32**, R25 (2006).

[4] L. Kluberg and H. Satz, in *Landolt-Börnstein–Group I Elementary Particles, Nuclei and Atoms*, edited by R. Stock, Relativistic Heavy Ion Physics Vol. 23 (Springer-Verlag, Berlin, Heidelberg, 2010).

[5] R. Rapp, D. Blaschke, and P. Crochet, Charmonium and bottomonium production in heavy-ion collisions, Prog. Part. Nucl. Phys. **65**, 209 (2010).

[6] J. Zhao, K. Zhou, S. Chen, and P. Zhuang, Heavy flavors under extreme conditions in high energy nuclear collisions, Prog. Part. Nucl. Phys. **114**, 103801 (2020).

[7] A. Mocsy, P. Petreczky, and M. Strickland, Quarkonia in the quark gluon plasma, Int. J. Mod. Phys. A **28**, 1340012 (2013).

[8] A. Rothkopf, Heavy quarkonium in extreme conditions, Phys. Rep. **858**, 1 (2020).

[9] F. Karsch, D. Kharzeev, and H. Satz, Sequential charmonium dissociation, Phys. Lett. B **637**, 75 (2006).

[10] P. P. Bhaduri, P. Hegde, H. Satz, and P. Tribedy, An Introduction to the Spectral Analysis of the QGP, in *The Physics of the Quark-Gluon Plasma*, Lecture Notes in Physics Vol. 785 (Springer, Berlin, 2010), p. 179.

[11] M. C. Abreu *et al.*, Evidence for deconfinement of quarks and gluons from the J/ψ suppression pattern measured in Pb-Pb collisions at the CERN SPS, Phys. Lett. B **477**, 28 (2000).

[12] R. Arnaldi *et al.*, J/ψ Production in Indium-Indium Collisions at 158 GeV/nucleon, Phys. Rev. Lett **99**, 132032 (2007).

[13] A. Adare *et al.*, J/ψ Production vs Centrality, Transverse Momentum, and Rapidity in Au+Au Collisions at $\sqrt{s_{NN}} = 200$ GeV, Phys. Rev. Lett. **98**, 232301 (2007).

[14] A. Adare *et al.*, J/ψ suppression at forward rapidity in Au+Au collisions at $\sqrt{s_{NN}}=200$ GeV, Phys. Rev. C **84**, 054912 (2011).

[15] J. Adam *et al.*, Measurement of inclusive J/ψ suppression in Au+Au collisions at $\sqrt{s_{NN}} = 200$ GeV through the dimuon channel at STAR, Phys. Lett. B **797**, 134917 (2019).

[16] B. B. Abelev *et al.*, Centrality, rapidity and transverse momentum dependence of J/ψ suppression in Pb-Pb collisions at $\sqrt{s_{NN}} = 2.76$ TeV, Phys. Lett. B **734**, 314 (2014).

[17] J. Adam *et al.*, Differential studies of inclusive J/ψ and ψ(2S) production at forward rapidity in Pb-Pb collisions at $\sqrt{s_{NN}} = 2.76$ TeV, J. High Energy Phys. 05 (2016) 179.

[18] J. Adam *et al.*, J/ψ suppression at forward rapidity in Pb-Pb collisions at $\sqrt{s_{NN}} = 5.02$ TeV, Phys. Lett. B **766**, 212 (2017).

[19] S. Chatrchyan *et al.*, Suppression of non-prompt J/ψ, prompt

J/ψ, and Y(1S) in PbPb collisions at $\sqrt{s_{NN}} = 2.76$ TeV, J. High Energy Phys. 05 (2012) 063.

[20] S. Acharya *et al.*, Studies of J/ψ production at forward rapidity in Pb-Pb collisions at $\sqrt{s_{NN}} = 5.02$ TeV, J. High Energy Phys. 02 (2020) 41.

[21] M. Aaboud *et al.*, Prompt and non-prompt J/ψ and $\psi(2S)$ suppression at high transverse momentum in 5.02 TeV Pb+Pb collisions with the ATLAS experiment, Eur. Phys. J. C **78**, 762 (2018).

[22] A. M. Sirunyan *et al.*, Relative Modification of Prompt $\psi(2S)$ and J/ψ Yields from pp to PbPb Collisions at $\sqrt{s_{NN}} = 5.02$ TeV, Phys. Rev. Lett. **118**, 162301 (2017).

[23] A. M. Sirunyan *et al.*, Measurement of prompt and nonprompt charmonium suppression in PbPb collisions at 5.02 TeV, Eur. Phys. J. C **78**, 509 (2018).

[24] ALICE Collaboration, $\psi(2S)$ suppression in Pb-Pb collisions at the LHC, arXiv:2210.08893.

[25] S. Chatrchyan *et al.*, Observation of Sequential Υ Suppression in PbPb Collisions, Phys. Rev. Lett. **109**, 222301 (2012); **120**, 199903(E) (2018).

[26] X. Du, M. He, and R. Rapp, Color screening and regeneration of bottomonia in high-energy heavy-ion collisions, Phys. Rev. C **96**, 054901 (2017).

[27] M. Gazdzicki and M. I. Gorenstein, Evidence for Statistical Production of J/ψ Mesons in Nuclear Collisions at the CERN SPS, Phys. Rev. Lett. **83**, 4009 (1999).

[28] K. A. Bugaev, M. Gazdzicki, and M. I. Gorenstein, Ω, J/ψ and ψ' transverse mass spectra at RHIC, Phys. Lett. B **544**, 127 (2002).

[29] A. Andronic, P. Braun-Munzinger, M. K. Köhler, K. Redlich, and J. Stachel, Transverse momentum distributions of charmonium states with the statistical hadronization model, Phys. Lett. B **797**, 134836 (2019).

[30] V. Khachatryan *et al.*, Suppression of $\Upsilon(1S)$, $\Upsilon(2S)$ and $\Upsilon(3S)$ production in PbPb collisions at $\sqrt{s_{NN}} = 2.76$ TeV, Phys. Lett. B **770**, 357 (2017).

[31] K. Reygers, A. Schmah, A. Berdnikova, and X. Sun, Blast-wave description of Υ elliptic flow at energies available at the CERN Large Hadron Collider, Phys. Rev. C **101**, 064905 (2020).

[32] S. Acharya *et al.*, Measurement of $\Upsilon(1S)$ Elliptic Flow at Forward Rapidity in Pb-Pb Collisions at $\sqrt{s_{NN}} = 5.02$ TeV, Phys. Rev. Lett. **123**, 192301 (2019).

[33] CMS Collaboration, Measurement of the elliptic flow of $\Upsilon(1S)$ and $\Upsilon(2S)$ mesons in PbPb collisions at $\sqrt{s_{NN}} = 5.02$ TeV, CERN Report No. CMS-PAS-HIN-19-002, 2019 (unpublished).

[34] S. Acharya *et al.*, J/ψ Elliptic Flow in Pb-Pb Collisions at $\sqrt{s_{NN}} = 5.02$ TeV, Phys. Rev. Lett. **119**, 242301 (2017).

[35] S. Acharya *et al.*, Study of J/ψ azimuthal anisotropy at forward rapidity in Pb-Pb collisions at $\sqrt{s_{NN}} = 5.02$ TeV, J. High Energy Phys. 02 (2019) 12.

[36] S. Acharya *et al.*, J/ψ elliptic and triangular flow in Pb-Pb collisions at $\sqrt{s_{NN}} = 5.02$ TeV, J. High Energy Phys. 10 (2020) 141.

[37] M. He, B. Wu, and R. Rapp, Collectivity of J/ψ Mesons in Heavy-Ion Collisions, Phys. Rev. Lett. **128**, 162301 (2022).

[38] P. P. Bhaduri, N. Borghini, A. Jaiswal, and M. Strickland, Anisotropic escape mechanism and elliptic flow of bottomonia, Phys. Rev. C **100**, 051901(R) (2019).

[39] P. P. Bhaduri, M. Alqahtani, N. Borghini, A. Jaiswal, and M. Strickland, Fireball tomography from bottomonia elliptic flow

in relativistic heavy-ion collisions, Eur. Phys. J. C **81**, 585 (2021).

[40] S. Gupta and R. Sharma, Thermalization of quarkonia at energies available at the CERN Large Hadron Collider, Phys. Rev. C **89**, 057901 (2014).

[41] A. Andronic, P. Braun-Munzinger, K. Redlich, and J. Stachel, Statistical hadronization of heavy quarks in ultra-relativistic nucleus-nucleus collisions, Nucl. Phys. A **789**, 334 (2007).

[42] A. Andronic, P. Braun-Munzinger, K. Redlich, and J. Stachel, Evidence for charmonium generation at the phase boundary in ultra-relativistic nuclear collisions, Phys. Lett. B **652**, 259 (2007).

[43] A. Andronic, P. Braun-Munzinger, M. K. Köhler, and J. Stachel, Testing charm quark thermalisation within the statistical hadronisation Model, Nucl. Phys. A **982**, 759 (2019).

[44] A. Andronic, P. Braun-Munzinger, K. Redlich, and J. Stachel, Decoding the phase structure of QCD via particle production at high energy, Nature (London) **561**, 321 (2018).

[45] S. Chatterjee, R. M. Godbole, and S. Gupta, Strange freezeout, Phys. Lett. B **727**, 554 (2013).

[46] P. Braun-Munzinger, J. Stachel, J. P. Wessels, and N. Xu, Thermal equilibration and expansion in nucleus-nucleus collisions at the AGS, Phys. Lett. B **344**, 43 (1995).

[47] J. Cleymans and K. Redlich, Chemical and thermal freeze-out parameters from 1A to 200A GeV, Phys. Rev. C **60**, 054908 (1999).

[48] F. Becattini, J. Manninen, and M. Gazdzicki, Energy and system size dependence of chemical freeze-out in relativistic nuclear collisions, Phys. Rev. C **73**, 044905 (2006).

[49] A. Andronic, P. Braun-Munzinger, and J. Stachel, Phys. Lett. B **673**, 142 (2009); Thermal hadron production in relativistic nuclear collisions: The Hadron mass spectrum, the horn, and the QCD phase transition, **678**, 516(E) (2009).

[50] V. Vovchenko, M. I. Gorenstein, and H. Stoecker, Finite resonance widths influence the thermal-model description of hadron yields, Phys. Rev. C **98**, 034906 (2018).

[51] N. Sarkar, P. Deb, and P. Ghosh, Finite size effect on thermodynamics of hadron gas in high-multiplicity events of proton-proton collisions at the LHC, arXiv:1905.06532.

[52] A. Andronic, P. Braun-Munzinger, J. Stachel, and M. Winn, Interacting hadron resonance gas meets lattice QCD, Phys. Lett. B **718**, 80 (2012).

[53] N. Sarkar and P. Ghosh, Thermalization in a small hadron gas system and high-multiplicity pp events, Phys. Rev. C **96**, 044901 (2017).

[54] P. A. Zyla *et al.* (Particle Data Group), Review of particle physics, Prog. Theor. Exp. Phys. **2020**, 083C01 (2020).

[55] P. Garg, D. K. Mishra, P. K. Netrakanti, B. Mohanty, A. K. Mohanty, B. K. Singh, and N. Xu, Conserved number fluctuations in a hadron resonance gas model, Phys. Lett. B **726**, 691 (2013).

[56] P. Alba, W. Alberico, R. Bellwied, M. Bluhm, V. M. Sarti, M. Nahrgang, and C. Ratti, Freeze-out conditions from net-proton and net-charge fluctuations at RHIC, Phys. Lett. B **738**, 305 (2014).

[57] S. Chatrchyan *et al.*, Event activity dependence of Y(nS) production in $\sqrt{s_{NN}} = 5.02$ TeV pPb and $\sqrt{s} = 2.76$ TeV pp collisions, J. High Energy Phys. 04 (2014) 103.

[58] S. Acharya *et al.*, Υ production and nuclear modification at forward rapidity in Pb–Pb collisions at $\sqrt{s_{NN}} = 5.02$ TeV, Phys. Lett. B **822**, 136579 (2021).

[59] A. M. Sirunyan *et al.*, Suppression of Excited Υ States Relative to the Ground State in Pb-Pb Collisions at $\sqrt{s_{NN}} = 5.02$ TeV, Phys. Rev. Lett. **120**, 142301 (2018).

[60] CMS Collaboration, Observation of the $\Upsilon(3S)$ meson and sequential suppression of Υ states in PbPb collisions at $\sqrt{s_{NN}} = 5.02$ TeV, CERN Report No. CMS-PAS-HIN-21-007, 2022 (unpublished).

[61] ATLAS Collaboration, Production of $\Upsilon(nS)$ mesons in Pb+Pb and *pp* collisions at 5.02 TeV, Phys. Rev. C **107**, 054912 (2023).

[62] A. M. Sirunyan *et al.*, Measurement of nuclear modification factors of $\Upsilon(1S)$, $\Upsilon(2S)$, and $\Upsilon(3S)$ mesons in PbPb collisions at $\sqrt{s_{NN}} = 5.02$ TeV, Phys. Lett. B **790**, 270 (2019).

[63] B. Aboona *et al.*, Observation of Sequential Υ Suppression in Au+Au Collisions at $\sqrt{s_{NN}} = 200$ GeV with the STAR Experiment, Phys. Rev. Lett. **130**, 112301 (2023).

[64] W. Zha, C. Yang, B. Huang, L. Ruan, S. Yang, Z. Tang, and Z. Xu, Systematic study of the experimental measurements on ratios of different Υ states, Phys. Rev. C **88**, 067901 (2013).

[65] B. Alessandro *et al.*, ψ' production in Pb-Pb collisions at 158 GeV/nucleon, Eur. Phys. J. C **49**, 559 (2007).

[66] V. Khachatryan *et al.*, Measurement of Prompt $\psi(2S) \to J/\psi$ Yield Ratios in Pb-Pb and *p-p* Collisions at $\sqrt{s_{NN}} = 2.76$ TeV, Phys. Rev. Lett. **113**, 262301 (2014).

[67] CMS Collaboration, Measurement of the $\psi(2S)$ meson in PbPb collisions at $\sqrt{s_{NN}} = 2.76$ TeV, CERN Report No. CMS-PAS-HIN-12-007, 2012 (unpublished).

[68] A. M. Sirunyan *et al.*, Measurement of prompt $\psi(2S)$ production cross sections in proton-lead and proton-proton collisions at $\sqrt{s_{NN}} = 5.02$ TeV, Phys. Lett. B **790**, 509 (2019).

[69] J. Adam *et al.*, Inclusive, prompt and non-prompt J/ψ production at mid-rapidity in Pb-Pb collisions at $\sqrt{s_{NN}} = 2.76$ TeV, J. High Energy Phys. 07 (2015) 0511.

[70] ALICE Collaboration, Prompt and non-prompt J/ψ production in Pb-Pb collisions at 5.02 TeV, QM2022, ALI-PREL-509318 (2022).

[71] A. M. Sirunyan *et al.*, Study of J/ψ meson production inside jets in pp collisions at $\sqrt{s} = 8$ TeV, Phys. Lett. B **804**, 135409 (2020).

[72] S. Acharya *et al.* (ALICE Collaboration), Measurements of inclusive J/ψ production at midrapidity and forward rapidity in Pb-Pb collisions at $\sqrt{s_{NN}} = 5.02$ TeV, arXiv:2303.13361.

[73] P. Braun-Munzinger and J. Stachel, (Non)thermal aspects of charmonium production and a new look at J/ψ suppression, Phys. Lett. B **490**, 196 (2000).

[74] R. L. Thews, M. Schroedter, and J. Rafelski, Enhanced J/ψ production in deconfined quark matter, Phys. Rev. C **63**, 054905 (2001).

[75] X. Du and R. Rapp, Sequential regeneration of charmonia in heavy-ion collisions, Nucl. Phys. A **943**, 147 (2015).

[76] M. I. Gorenstein, K. A. Bugaev, and M. Gazdzicki, Ω, J/ψ, and ψ' Production in Nuclear Collisions and Quark-Gluon-Plasma Hadronization, Phys. Rev. Lett. **88**, 132301 (2002).

[77] A. M. Sirunyan *et al.*, Investigation into the event-activity dependence of $\Upsilon(nS)$ relative production in proton-proton collisions at $\sqrt{s} = 7$ TeV, J. High Energy Phys. 11 (2020) 001.

[78] T. Chowdhury, Study of Υ production as a function of charged-particle multiplicity in proton-proton collisions at $\sqrt{s} = 13$ TeV

with ALICE at the LHC, Ph.D. thesis, Clermont-Ferrand University, 2019 (unpublished).

[79] S. Acharya *et al.*, Υ production in p–Pb collisions at $\sqrt{s_{NN}} = 8.16$ TeV, Phys. Lett. B **806**, 135486 (2020).

[80] S. Acharya *et al.*, Inclusive quarkonium production in pp collisions at $\sqrt{s} = 5.02$ TeV, Eur. Phys. J. C **83**, 61 (2023).

[81] B. B. Abelev *et al.*, Measurement of quarkonium production at forward rapidity in *pp* collisions at $\sqrt{s} = 7$ TeV, Eur. Phys. J. C **74**, 2974 (2014).

[82] J. Adam *et al.*, Inclusive quarkonium production at forward rapidity in pp collisions at $\sqrt{s} = 8$ TeV, Eur. Phys. J. C **76**, 184 (2016).

[83] S. Acharya *et al.*, Energy dependence of forward-rapidity J/ψ and $\psi(2S)$ production in pp collisions at the LHC, Eur. Phys. J. C **77**, 392 (2017).

[84] J. Adam *et al.*, Centrality dependence of $\psi(2S)$ suppression in *p*-Pb collisions at $\sqrt{s_{NN}} = 5.02$ TeV, J. High Energy Phys. 06 (2016) 050.

[85] B. B. Abelev *et al.*, Suppression of $\psi(2S)$ production in *p*-Pb collisions at $\sqrt{s_{NN}} = 5.02$ TeV, J. High Energy Phys. 12 (2014) 073.

[86] S. Acharya *et al.*, Centrality dependence of J/ψ and $\psi(2S)$ production and nuclear modification in *p*-Pb collisions at $\sqrt{s_{NN}} = 8.16$ TeV, J. High Energy Phys. 02 (2021) 002.

[87] S. Acharya *et al.*, Measurement of nuclear effects on $\psi(2S)$ production in *p*-Pb collisions at $\sqrt{s_{NN}} = 8.16$ TeV, J. High Energy Phys. 07 (2020) 237.

[88] V. Khachatryan *et al.*, Observation of long-range near-side angular correlations in proton-proton collisions at the LHC, J. High Energy Phys. 09 (2010) 091.

[89] V. Khachatryan *et al.*, Measurement of Long-Range Near-Side Two-Particle Angular Correlations in *pp* Collisions at $\sqrt{s} = 13$ TeV, Phys. Rev. Lett. **116**, 172302 (2016).

[90] S. Chatrchyan *et al.*, Observation of long-range near-side angular correlations in proton-lead collisions at the LHC, Phys. Lett. B **718**, 795 (2013).

[91] R. Aaij *et al.*, Measurements of long-range near-side angular correlations in $\sqrt{s_{NN}} = 5$ TeV proton-lead collisions in the forward region, Phys. Lett. B **762**, 473 (2016).

[92] V. Khachatryan *et al.*, Evidence for collectivity in pp collisions at the LHC, Phys. Lett. B **765**, 193 (2017).

[93] G. Aad *et al.*, Observation of Long-Range Elliptic Azimuthal Anisotropies in $\sqrt{s} = 13$ and 2.76 TeV *pp* Collisions with the ATLAS Detector, Phys. Rev. Lett. **116**, 172301 (2016).

[94] R. Aaij *et al.*, Study of J/ψ production and cold nuclear matter effects in *p*Pb collisions at $\sqrt{s_{NN}} = 5$ TeV, J. High Energy Phys. 02 (2014) 072.

[95] R. Aaij *et al.*, Prompt and nonprompt J/ψ production and nuclear modification in *p*Pb collisions at $\sqrt{s_{NN}} = 8.16$ TeV, Phys. Lett. B **774**, 159 (2017).

[96] S. Acharya *et al.*, Prompt and non-prompt J/ψ production cross sections at midrapidity in proton-proton collisions at $\sqrt{s} = 5.02$ and 13 TeV, J. High Energy Phys. 03 (2022) 190.

[97] G. Aad *et al.*, Measurement of the differential cross-sections of prompt and non-prompt production of J/ψ and $\psi(2S)$ in *pp* collisions at $\sqrt{s} = 7$ and 8 TeV with the ATLAS detector, Eur. Phys. J. C **76**, 283 (2016).